Journal of Nuclear Medicine, published on March 10, 2022 as doi:10.2967/jnumed.122.263884

^{68}Ga-Citrate Positron Emission Tomography of Healthy Men: Whole-Body Biodistribution Kinetics and Radiation Dose Estimates

Sami Suilamo[1,2], Xiang-Guo Li[3,4,5], Petteri Lankinen[6,7], Vesa Oikonen[3], Tuula Tolvanen[1,7], Pauliina Luoto[3,7], Riikka Viitanen[3], Antti Saraste[3,7,8], Marko Seppänen[7,9], Laura Pirilä[10,11], Ulla Hohenthal[12], and Anne Roivainen[3,5,7]

[1]Department of Medical Physics, Turku University Hospital, Turku, Finland; [2]Department of Oncology and Radiotherapy, Turku University Hospital, Turku, Finland; [3]Turku PET Centre, University of Turku, Turku, Finland; [4]Department of Chemistry, University of Turku, Turku, Finland; [5]InFLAMES Research Flagship Center, University of Turku, Turku, Finland; [6]Department of Orthopaedics and Traumatology, Turku University Hospital and University of Turku, Turku, Finland; [7]Turku PET Centre, Turku University Hospital, Turku, Finland; [8]Heart Center, Turku University Hospital, Turku, Finland; [9]Department of Clinical Physiology and Nuclear Medicine, Turku University Hospital, Turku, Finland; [10]Department of Rheumatology and Clinical Immunology, Division of Medicine, Turku University Hospital; Turku, Finland; [11]Department of Medicine, University of Turku, Turku, Finland; [12]Department of Infectious Diseases, Division of Medicine, Turku University Hospital, Turku, Finland.

Correspondence: Prof. Anne Roivainen, PhD, Turku PET Centre, Kiinamyllynkatu 4-8, FI-20521 Turku, Finland. Tel: +35823132862, Fax: +35822318191, E-mail: anne.roivainen@utu.fi

First author: Medical Physicist Sami Suilamo, Lic.Phil., Turku University Hospital, Kiinamyllynkatu 4-8, FI-20521 Turku, Finland. Tel: +35823130708, E-mail: sami.suilamo@tyks.fi

Word count: 4656; abstract word count 346

Running title: Kinetics and dosimetry of ^{68}Ga-citrate

Conflict of interest: The authors have no conflicts of interest to disclose.

Financial support: The study was conducted within the Finnish Centre of Excellence in Cardiovascular and Metabolic Diseases, supported by the Academy of Finland, University of Turku, Turku University Hospital, and Åbo Akademi University. The study was financially supported by grants from the State Research Funding of Turku University Hospital, and the Sigrid Jusélius Foundation.

ABSTRACT

^{68}Ga-citrate has one of the simplest chemical structures of all ^{68}Ga-radiopharmaceuticals, and its clinical use is justified by the proven medical applications using its isotope-labeled compound ^{67}Ga-citrate. To support broader application of ^{68}Ga-citrate in medical diagnosis, further research is needed to gain clinical data from healthy volunteers. In this work, we studied the biodistribution of ^{68}Ga-citrate and subsequent radiation exposure from it in healthy males.

Methods: ^{68}Ga-citrate was prepared with an acetone-based radiolabeling procedure compliant with Good Manufacturing Practices. Six healthy males (age 41 ± 12 years, mean ± SD) underwent sequential whole-body PET/CT scans after an injection of 204 ± 8 MBq of ^{68}Ga-citrate. Serial arterialized venous blood samples were collected during PET imaging and the radioactivity concentration was measured with a gamma counter. Urinary voids were collected and measured. The Medical Internal Radiation Dose (MIRD) bladder-voiding model with a 3.5 hour voiding interval was used. A model using a 70 kg adult male and MIRD schema was used to estimate absorbed doses in target organs and effective doses. Calculations were performed using OLINDA/EXM 2.0 software.

Results: Radioactivity clearance from the blood was slow, and relatively high radioactivity concentrations were observed over the whole of the 3 hour measuring period. Although radioactivity excretion via urine was rather slow (biological half-time, 69 ± 24 hours), the highest decay-corrected concentrations in urinary bladder contents were measured at 90 and 180 minute time points. Moderate concentrations were also seen in kidneys, liver, and spleen. The source organs showing the largest residence times were muscle, liver, lung, and heart contents. The heart wall received the highest absorbed dose of 0.077 ± 0.008 mSv/MBq. The mean effective dose (ICRP 103) was 0.021 ± 0.001 mSv/MBq.

Conclusion: PET imaging with ^{68}Ga-citrate is associated with modest radiation exposure. A 200 MBq injection of ^{68}Ga-citrate results in an effective radiation dose of 4.2 mSv, which is in the same range as

other ^{68}Ga-labeled tracers. This suggests the feasibility of clinical studies using ^{68}Ga-citrate imaging in humans and the possibility of performing multiple scans in the same subjects across the course of a year.

Key Words: biodistribution; ^{68}Ga-citrate; PET; pharmacokinetics; radiation dose

INTRODUCTION

Gallium-68 (^{68}Ga) is a transition metal that can be used for positron emission tomography (PET) imaging as ^{68}Ga-citrate or ^{68}Ga-chloride, and also in its chelated forms with biomolecules (e.g., chelator-conjugated peptides). ^{68}Ga-labeled pharmaceuticals are frequently used in nuclear medicine, and can be conveniently manufactured with kits and fully automated commercially available devices (*1*). ^{68}Ga-citrate is one such ^{68}Ga-radiopharmaceutical that has entered the clinical trial stage, and its use in PET is based on Ga^{3+} uptake and transportation mechanisms. Ga^{3+} is considered an analogue of Fe^{3+}, and binds to transferrin and other biomolecules *in vivo*. Although only a few human studies using ^{68}Ga-citrate PET have been performed (*2–13*), ^{68}Ga-citrate has already been shown to be a sensitive and specific PET tracer for the imaging of infection and inflammation, including inflammatory bowel disease (*3*), bone infection (*4*), intra-abdominal infection (*5*), and prosthetic joint infection (*12*). In addition, we recently observed unexpectedly high ^{68}Ga-citrate accumulation in atherosclerotic lesions in patients with *Staphylococcus aureus* bacteremia (*8*). Furthermore, patients with high-grade glioma, hepatocellular carcinoma and prostate cancer have been imaged with ^{68}Ga-citrate according to the hypothesis that Ga^{3+} uptake should increase in these tumors because of upregulated activity of transferrin receptor (*7, 9–11*). Evidence from clinical and preclinical investigations (*7, 14, 15*) suggests that ^{68}Ga-citrate has potential in a number of clinical applications, and that further research is warranted.

The purpose of this clinical study was to determine the biodistribution of intravenously administered ^{68}Ga-citrate in healthy male volunteers. This information will help to determine the optimal PET protocol for ^{68}Ga-citrate imaging of inflammatory and infectious diseases, and cancer. The whole-body imaging should allow identification of those organs that are most exposed to ionizing radiation and allow calculation of the dose absorbed by each organ.

MATERIALS AND METHODS

Chemicals and Reagents

All chemicals were purchased from commercial sources and were reagent, analytical, ultrapure, or European Pharmacopeia grade.

Preparation of ^{68}Ga-Citrate

^{68}Ga-citrate (Fig. 1A) was produced according to an established protocol (*3*). Aqueous hydrochloric acid (0.1 M, 6 mL) was used to elute ^{68}Ga-radioactivity from a ^{68}Ge/^{68}Ga-generator (IGG-100, 1850 MBq, Eckert & Ziegler Isotope Products, Valencia, CA, USA), and the ^{68}Ga-eluate was passed through a cation-exchange cartridge (Strata X-C, Phenomenex Inc., Torrance, CA, USA). The retained ^{68}Ga was eluted into a reaction vial with acidified acetone (800 µL, containing 0.02 M HCl and 3.25% water). The acetone was removed by evaporation for 4 minutes at 110ºC and sodium citrate buffer (4 mL) was added. After 4 minutes, the reaction mixture was sterile-filtrated into an end product vial and diluted with saline (9 mg/mL, 6 mL). Radiochemical purity was measured by instant thin layer chromatography (iTLC) with methanol/acetic acid (9:1, *v*/*v*) as a mobile phase.

Subjects

Six healthy male volunteers (age, 41 ± 13 years; weight, 75 ± 4 kg; height, 177 ± 4 cm) participated in this trial. ^{68}Ga-citrate was injected via a catheter inserted into an antecubital vein and blood samples were drawn through another catheter inserted into the contralateral arm.

Before starting this clinical trial, approvals were obtained from the joint Ethics Committee of the University of Turku and Turku University Hospital, as well as the Finnish Medicines Agency. Full

informed written consent was obtained from all subjects beforehand. This study is registered at ClinicalTrials.gov (NCT01951300).

Questionnaires were used to assess the absence of significant medical, neurological, and psychiatric history, and any history of alcohol or drug abuse. In addition, routine blood tests, electrocardiography, a physical examination, and a review of medical history were performed for each subject.

PET/CT Imaging

The biodistribution of ^{68}Ga-citrate was imaged using a GE Discovery 690 PET/computed tomography (CT) scanner (General Electric Medical Systems, Milwaukee, WI, USA). This scanner combines 64-slice CT with PET acquired using 24 rings of lutetium-yttrium-orthosilicate (LYSO) detectors, which provide 47 imaging planes with an axial field of view (FOV) of 15.7 cm. A low-dose CT for attenuation correction and anatomical reference was acquired before PET, using a voltage of 120 kV and current of 10 mA. Whole-body PET acquisitions were made 1, 5, 10, 20, 30, 90, and 180 minutes after an i.v. injection of 204 ± 8 MBq of ^{68}Ga-citrate. The acquisition times per bed position were 20, 30, 65, 65, 120, 240, and 240 s, respectively. The scanning at 90 minutes post-injection included 14 bed positions covering the range from the head to the toes, whereas all other scans used only eight bed positions covering the range from the head to mid thighs.

PET images were reconstructed using a time-of-flight 3D VUE Point algorithm with two iterations, 24 subsets, and a 6.4 mm full width at half maximum post-filter. Scatter correction, random counts, and dead-time corrections were all incorporated into the reconstruction algorithm. The final matrix size was 192 × 192 × 47 voxels. The plane thickness of the PET scanner was 3.27 mm, and the axial spatial

resolution for 3D mode was 4.74 mm at full width at half maximum at a 1 cm offset from the center of the FOV (*16*).

Blood and Urine Measurements

Serial arterialized (the arm was heated with a wrapped heating pad) venous blood samples were collected into heparinized tubes at 1, 5, 10, 20, 30, 60, 90, 180, and 240 minutes after the injection of ^{68}Ga-citrate. The radioactivity of the whole blood was measured with an automatic gamma counter (1480 Wizard 3"; EG&G Wallac, Turku, Finland). Plasma was separated by centrifugation (2,100 ×*g* for 5 minutes at 4°C) and the plasma radioactivity was measured. The plasma concentration C_0 was estimated by fitting a monoexponential function to the plasma concentrations collected between 5 and 30 minutes.

The subjects were asked to urinate during two breaks in the PET imaging session and again after the session. The mean times for urination were 61 minutes after injection, 163 minutes after injection, and 218 minutes after injection. Urinary voids were collected, the total volume was measured, and a 2.5 mL sample was taken for radioactivity measurement with a VDC 405 dose calibrator (Veenstra Instruments, Joure, The Netherlands).

Distribution Kinetics and Radiation Dose Estimates

Eclipse 13.6 software (Varian Medical Systems, Helsinki, Finland) was used to define the radioactivity concentrations of the source organs at different time points. The source organ volumes were either defined on CT images or the volumes of the organs of the Reference Male (*17*) were used.

Residence times in source organs were calculated from area under the time-activity curves. The curves were defined by fitting a sum of two exponential functions. The Medical Internal Radiation Dose (MIRD) bladder-voiding model (*18*) with a 3.5 hour voiding interval was used. A model with a 70 kg

adult male and MIRD schema (*19*) was used to estimate the absorbed doses in the target organs and the effective doses. Calculations were performed using OLINDA/EXM 2.0 software (Organ Level INternal Dose Assessment/EXponential Modeling, Radar, USA). In addition, OLINDA 1.0 results were calculated.

RESULTS

Radiochemistry

The manufactured ^{68}Ga-citrate fulfilled all the product quality specifications (Supplemental Table 1) for clinical use. The radiochemical purity was ≥ 95%, pH was in the range of 3.0−7.0, and the acetone content was ≤ 0.5%. An example iTLC plot used to determine radiochemical purity is shown in Figure 1B.

Biodistribution and Biokinetics

Whole-body dynamic PET/CT imaging data was obtained from six subjects over a period of 180 minutes after ^{68}Ga-citrate administration. Figure 2 shows representative images from a subject. The radioactivity concentrations in 20 organs/tissues of interest were quantified at time points of 1, 5, 10, 20, 30, 90, and 180 minutes, and the results are presented in Supplemental Table 2. At 30 minutes post-injection, standardized uptake ratios (SUVs) in the brain, heart contents, kidneys, liver, trabecular bone, and red marrow were 0.26 ± 0.04 (mean ± SD), 5.16 ± 0.48, 3.15 ± 0.46, 2.78 ± 0.25, 0.70 ± 0.15, and 1.80 ± 0.12, respectively. Figure 3 shows time-activity curves (TACs) for the 20 organs/tissues, revealing the whole-body distribution kinetics of radioactivity over the 180 minutes after ^{68}Ga-citrate administration.

The mean voided radioactivity at a mean void time of 61 minutes after injection (during a break between PET imaging session) was 1.76 ± 0.47 percentage of the injected radioactivity dose (%ID; Fig.

4). All six subjects were able to urinate during the first PET imaging session break, three were able to urinate between imaging session 2 and 3, and two after the complete imaging session.

Radioactivity clearance from the blood was slow (Fig. 5). The estimated concentration value at t = 0 (representing C_0) in SUV units was 17.3 ± 1.8 g/mL (Supplemental Table 3). The inverse of C_0, which is related to the total plasma volume, was 0.059 ± 0.006 L/kg. The plasma concentration at 4 hours (*n* = 5) was 5.8 ± 0.6 g/mL, and its inverse, which may be related to the extracellular volume of the body, was 0.17 ± 0.02 L/kg.

Residence Times and Radiation Dose Estimates

The residence times (normalized numbers of disintegrations) were determined for the source organs and the remainder of the body of each subject, and their mean ± SD, range, and coefficient of variation (COV) are listed in Table 1. The COV values were in the range of 4–49%. The largest residence times were in muscle (0.365 ± 0.043 hours), liver (0.091 ± 0.017 hours), lungs (0.079 ± 0.008 hours), and heart contents (0.048 ± 0.006 hours).

The organ dose estimates (given in Table 2) were calculated for a 70 kg adult male. The organs with the highest doses were the heart wall (0.077 ± 0.008 mSv/MBq), urinary bladder wall (0.039 ± 0.010 mSv/MBq), kidneys (0.036 ± 0.004 mSv/MBq), and lungs (0.036 ± 0.003 mSv/MBq). The lowest dose was in the brain (0.004 ± 0.001 mSv/MBq). The mean effective dose (ICRP 103) (*20*) was 0.021 ± 0.001 mSv/MBq. Thus, the effective dose from 200 MBq of injected radioactivity of ^{68}Ga-citrate was 4.2 mSv.

Organ dose estimates according to OLINDA 1.0 are presented in the Supplemental Table 4.

DISCUSSION

We previously studied ^{68}Ga-citrate in experimental disease models, as well as in patients with infections (*8*, *15*, *21*). This study is a basic investigation in healthy humans to collect data on whole-body distribution kinetics and radiation dose estimates, which will be useful in planning future clinical trials with ^{68}Ga-citrate.

Preparation of ^{68}Ga-Citrate

The radiopharmaceutical ^{68}Ga-citrate was produced using a straightforward protocol (*3*). The acetone-based cation-exchange cartridge elution method is an effective option for concentrating ^{68}Ga-radioactivity eluted from a generator (*1*). In our hospital, this method is used to manufacture three radiopharmaceuticals, including ^{68}Ga-citrate, in a fully automated manner. Citrate is a natural ligand that can coordinate to some metal ions, including gallium. Because of the nature of the nuclear physics of ^{68}Ga, the molarity of ^{68}Ga in a batch of eluate from a ^{68}Ge/^{68}Ga-generator is tiny. By contrast, the molarity of citrate (0.14 mmol) is in very great excess to ensure efficient coordination, which is neither feasible nor typical in the production of many other ^{68}Ga-radiopharmaceuticals. In this sense, citrate acts also as a vehicle, in addition to its role as a chelator. On iTLC, the chromatography behaviors of ^{68}Ga-citrate and free ^{68}Ga show a clear difference (Fig. 1B); free ^{68}Ga remains at the baseline while ^{68}Ga-citrate migrates up on the iTLC with a retention factor of 0.93. As there is not a citrate dose limit set in the European Pharmacopeia, quantification of the citrate in the end product formulation is not relevant in the quality control procedure.

PET Imaging and Biodistribution

In a typical ^{68}Ga-radiopharmaceutical, the ^{68}Ga-radionuclide is attached to a targeting molecule, for example a peptide, and the targeting molecule takes the radioactivity to the specific organs and tissues to be imaged. In the case of ^{68}Ga-citrate, the imaging and biodistribution is most probably based on the

biological mechanisms of $^{68}Ga^{3+}$, which can be chelated *in vivo* with biomolecules including ferritins (*13*). This implies that *in vivo* transmetalation takes place, even though citrate has sufficient strength to coordinate $^{68}Ga^{3+}$ in the manufacturing procedures. However, comparison studies have indicated that the imaging performance of ^{68}Ga-citrate is better than that of intravenously injected ^{68}Ga-chloride, at least as far as the limited available evidence shows (*15*), which might be an indication that citrate plays a role as a vehicle in the *in vivo* biodistribution. In this study, particular care was taken to ensure that the ^{68}Ga-citrate injection did not involve any Ga colloids, which usually accompany the ^{68}Ge/^{68}Ga-generator eluate or are formed if injected as ^{68}Ga-chloride.

For the PET imaging, each subject was intravenously administered 204 ± 8 MBq of ^{68}Ga-citrate. In a routine PET procedure performed in our hospital, for example, one using the standard tracer 2-deoxy-2-^{18}F-fluoro-*D*-glucose, the typical radioactivity dose is 4 MBq/kg of body weight. In this study, we used 204 ± 8 MBq (2.7 ± 0.2 MBq/kg) of ^{68}Ga-citrate per subject, which is in the typical dose range of our ^{68}Ga-radiopharmaceutical PET studies. The mass of gallium injected was negligible. It is noteworthy that when gallium is administered as a drug in high doses, it is known that the biodistribution changes (*22, 23*).

The sequential whole-body imaging was performed for 180 minutes to monitor the tracer kinetics *in vivo*. For visualization purposes, we prepared representative PET/CT images from a 22-year-old man and scaled the SUVs from 1 to 3 (Fig. 2). These images clearly show that the radioactivity concentration was much higher in heart, liver, lungs, and kidneys than in other organs. At a time point of 180 minutes post-injection, the whole-body radioactivity concentration became very low, which is an indication of sufficient data collection time range. To further quantify the radioactivity concentration in the 20 organs of interest, TACs were drawn from time 0 to 180 minutes post-administration (Fig. 3). Among the organs and tissues, the TACs from gall bladder, lower large intestine (left colon & rectum),, testes, and upper large intestines (right colon) were still increasing slightly at 180 minutes. It was not clear what factors

might have caused the slight accumulations in these organs. In cortical bone, red marrow, small intestine, and trabecular bone, the TACs showed a steady radioactivity residence along with time. In the urinary bladder, the general trend of radioactivity development was an initial increase then a decrease. In the rest of the organs, the TACs decreased to varying extents over the time period.

The radioactivity concentration in plasma stayed at a high level (Fig. 5), similar to that reported previously for the ^{68}Ge/^{68}Ga-generator eluate ^{68}Ga-chloride in a study on rats (*24*); the very slow decrease at 3–4 hours prevents reliable estimation of the total area-under-the-curve (from time zero to infinity) and total clearance. In previous animal studies, we found that the *in vivo* kinetics of ^{68}Ga-citrate and ^{68}Ga-chloride differed, possibly because the chelating properties of citrate prevent the precipitation of $^{68}Ga(OH)_3$ (*15*).

Radiation Dose Estimates

To determine the radiation burden, we analyzed the kinetics of radioactivity concentration in the main organs of healthy men up to 3 hours after an intravenous bolus injection of ^{68}Ga-citrate. In addition to the SD and range, the COV was used to indicate the precision and repeatability of the measurements among the six subjects. Our results revealed that the heart wall received the highest radiation dose, followed by the urinary bladder wall. This may be partially due to the relatively slow blood clearance and urinary excretion as the main clearance route. However, the relatively slow blood clearance was not a problem for target visualization in previous studies. The organ with the lowest radiation exposure was the brain (0.004 ± 0.001 mSv/MBq). Overall, the effective dose of ^{68}Ga-citrate (0.021 ± 0.001 mSv/MBq) was comparable to that of widely-used PET tracers including ^{68}Ga-DOTANOC (0.025 mSv/MBq) (*25*) and ^{18}F-FDG (0.019 mSv/MBq) (*26*). For example, a 200 MBq dose of ^{68}Ga-citrate may result in an effective dose of 4.2 ± 0.2 mSv.

CONCLUSION

The radiation burden from administration of ^{68}Ga-citrate for PET imaging is comparable with that of other commonly used ^{68}Ga-radiopharmaceuticals. The low radiation exposure of ^{68}Ga-citrate would allow for studies with multiple scans in the same individuals over the course of a year.

DISCLOSURE

The authors declare that they have no conflicts of interest relevant to this article.

ACKNOWLEDGMENTS

The authors thank the technical and nursing staff at Turku PET Centre for their assistance in this work. The authors thank Timo Kattelus for preparing figures.

KEY POINTS

QUESTION: What are the distribution kinetics of ^{68}Ga-citrate in healthy humans and what is the radiation burden resulting from its administration?

PERTINENT FINDINGS: Six healthy men underwent dynamic whole-body PET/CT imaging with blood and urine measurements. ^{68}Ga-citrate showed slow clearance from the blood circulation through renal excretion. The highest radiation exposure was to the heart wall. The effective dose of 0.021 mSv/MBq is similar to that of other commonly used ^{68}Ga-tracers.

IMPLICATIONS FOR PATIENT CARE: The characteristics of ^{68}Ga-citrate are favorable for human studies involving multiple scans in the same subject over the course of a year.

REFERENCES

1. Käkelä M, Luoto P, Viljanen T, et al. Adventures in radiosynthesis of clinical grade [^{68}Ga]Ga-DOTA-Siglec-9. *RSC Advances*. 2018;8:8051–8056.
2. Mintun MA, Dennis DR, Welch MJ, Mathias CJ, Schuster DP. Measurements of pulmonary vascular permeability with PET and gallium-68 transferrin. *J Nucl Med.* 1987;28:1704–1716.
3. Rizzello A, Pierro DD, Lodi F, et al. Synthesis and quality control of ^{68}Ga citrate for routine clinical PET. *Nucl Med Commun*. 2009;30:542–545.
4. Nanni C, Errani C, Boriani L, et al. ^{68}Ga-Citrate PET/CT for evaluating patients with infections of the bone: preliminary results. *J Nucl Med*. 2010;51:1932–1936.
5. Kumar V, Boddeti DK, Evans SG, Angelides S. ^{68}Ga-Citrate-PET for diagnostic imaging of infection in rats and for intra-abdominal infection in a patient. *Curr Radiopharm*. 2012;5:71–75.
6. Vorster M, Maes A, Jacobs A, et al. Evaluating the possible role of ^{68}Ga-citrate PET/CT in the characterization of indeterminate lung lesions. *Ann Nucl Med*. 2014;28:523–530.
7. Behr SC, Aggarwal R, Seo Y, et al. A Feasibility study showing [^{68}Ga]citrate PET detects prostate cancer. *Mol Imaging Biol.* 2016;18:946–951.
8. Salomäki SP, Kemppainen J, Hohenthal U, et al. Head-to-head comparison of ^{68}Ga-citrate and ^{18}F-FDG PET/CT for detection of infectious foci in patients with Staphylococcus aureus bacteraemia. *Contrast Media Mol Imaging.* 2017;2017:3179607.
9. Aggarwal R, Behr SC, Paris PL, et al. Real-time transferrin-based PET detects MYC-positive prostate cancer. *Mol Cancer Res.* 2017;15:1221–1229.
10. Aparici CM, Behr SC, Seo Y, et al. Imaging hepatocellular carcinoma with ^{68}Ga-citrate PET: first clinical experience. *Mol Imaging*. 2017;16: 1536012117723256.

11. Behr SC, Villanueva-Meyer JE, Li Y, et al. Targeting iron metabolism in high-grade glioma with ^{68}Ga-citrate PET/MR. *JCI Insight*. 2018;3:e93999.

12. Tseng JR, Chang YH, Yang LY, et al. Potential usefulness of ^{68}Ga-citrate PET/CT in detecting infected lower limb prostheses. *EJNMMI Res*. 2019;9:2.

13. Xu T, Chen Y. Research progress of [^{68}Ga]Citrate PET's utility in infection and inflammation imaging: a review. *Mol Imaging Biol*. 2020;22:22–32.

14. Nielsen OL, Afzelius P, Bender D, et al. Comparison of autologous ^{111}In-leukocytes, ^{18}F-FDG, ^{11}C-methionine, ^{11}C-PK11195 and ^{68}Ga-citrate for diagnostic nuclear imaging in a juvenile porcine *aureus osteomyelitis* model. *Am J Nucl Med Mol Imaging* 2015;5:169–182.

15. Lankinen P, Noponen T, Autio A, et al. A comparative ^{68}Ga-citrate and ^{68}Ga-chloride PET/CT imaging of Staphylococcus aureus osteomyelitis in the rat tibia. *Contrast Media Mol Imaging.* 2018;2018:9892604.

16. Bettinardi V, Presotto L, Rapisarda E, Picchio L, Gianolli L, Gilardi MC. Physical performance of the new hybrid PET/CT Discovery-690. *Med Phys*. 2011;38:5394–5411.

17. International Commission on Radiological Protection. Basic Anatomical and Physiological Data for Use in Radiological Protection: Reference Values. *ICRP Publication 89*. Oxford, UK: Pergamon Press; 2002.

18. Thomas SR, Stabin MG, Chin-Tu C, Samaratunga RC. MIRD pamphlet no. 14 revised: a dynamic urinary bladder model for radiation dose calculations. *J Nucl Med*. 1999;40(suppl):102S–123S.

19. Siegel JA, Thomas SR, Stubbs JB, et al. MIRD pamphlet no. 16: Techniques for quantitative radiopharmaceutical biodistribution data acquisition and analysis for use in human radiation dose estimates. *J Nucl Med*. 1999;40 (suppl):37S–61S.

20. ICRP Publication 103: The 2007 recommendations of the international commission on radiological protection. *Ann ICRP*. 2007;37:1–333.

21. Aro E, Seppänen M, Mäkelä KT, Luoto P, Roivainen A, Aro HT. PET/CT to detect adverse reactions to metal debris in patients with metal-on-metal hip arthroplasty: an exploratory prospective study. *Clin Physiol Funct Imaging.* 2018;38:847–855.

22. Bernstein LR. Mechanisms of therapeutic activity for gallium. *Pharmacol Rev.* 1998;50:665–682.

23. Aridis Pharmaceuticals. AR-501 (Gallium Citrate): Novel anti-infective for the growing problem of antibiotic resistance. https://www.aridispharma.com/ar-501/ Accessed January 26, 2022.

24. Autio A, Virtanen H, Tolvanen T, et al. Absorption, distribution and excretion of intravenously injected ^{68}Ge/^{68}Ga generator eluate in healthy rats, and estimation of human radiation dosimetry. *EJNMMI Res*. 2015;5:40.

25. Pettinato C, Sarnelli A, Di Donna M, et al. ^{68}Ga-DOTANOC: biodistribution and dosimetry in patients affected by neuroendocrine tumors. *Eur J Nucl Med Mol Imaging.* 2008;35:72–79.

26. ICRP Publication 80. Recalculated dose data for 19 frequently used radiopharmaceuticals from ICRP publication 53. *Ann ICRP*. 1998;28:47–83.

27. ICRP Publication 60: Recommendation of the international commission on radiological protection. *Ann ICRP*. 1991;21:493–502.

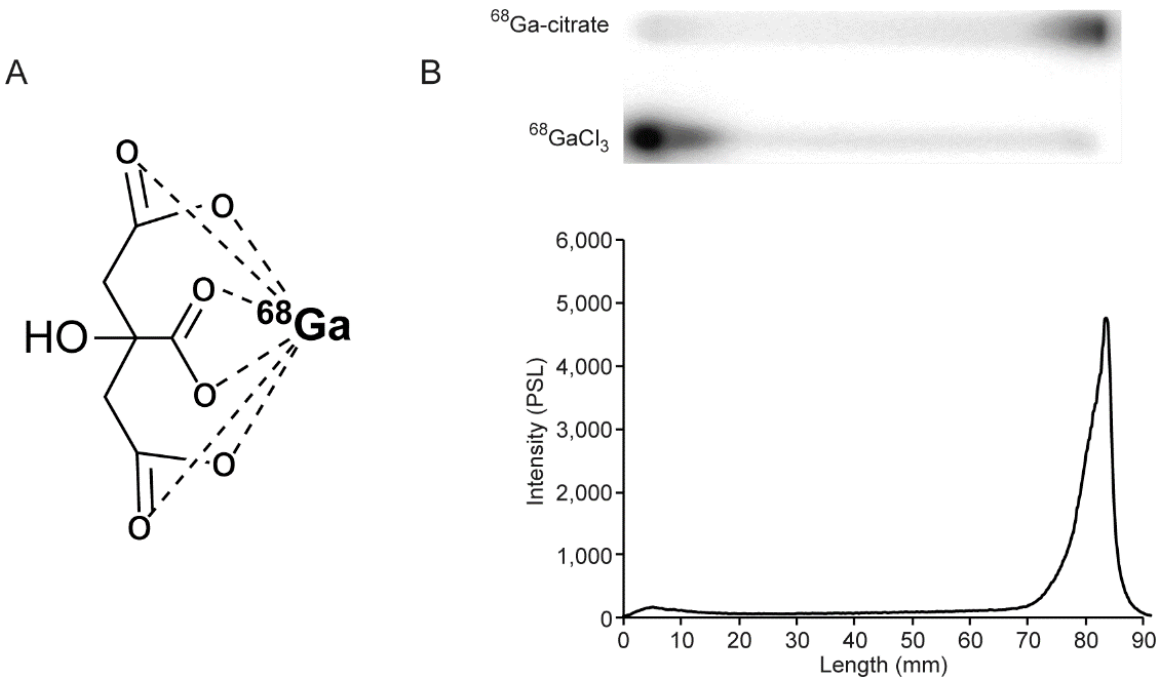

FIGURE 1. (A) Chemical structure of ^{68}Ga-citrate. (B) Quality control of ^{68}Ga-citrate with instant thin-layer chromatography developed using methanol/acetic acid (9:1, *v*/*v*) as a mobile phase and visualized and quantified by autoradiography.

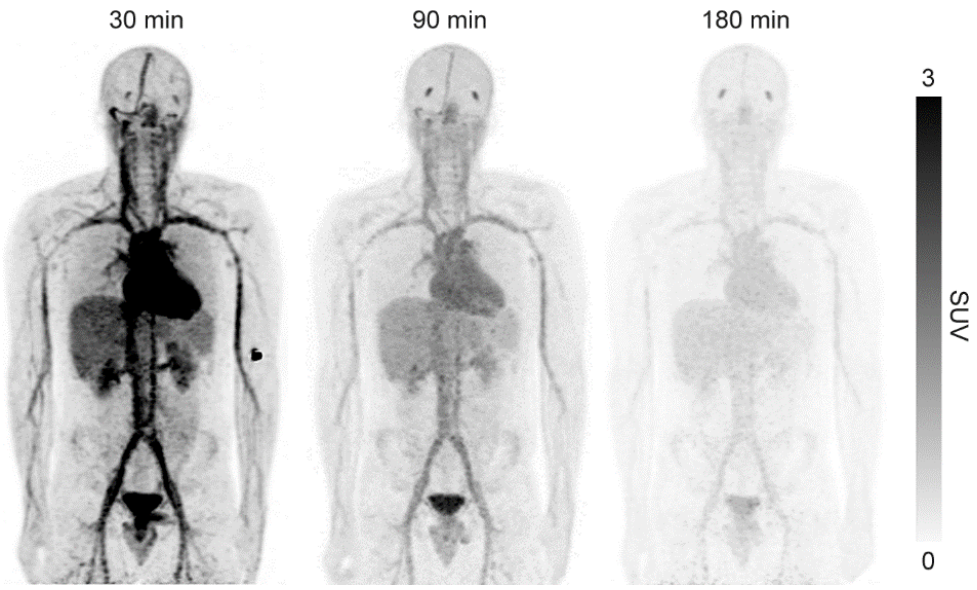

FIGURE 2. Whole-body distribution of 195 MBq of ^{68}Ga-citrate in a healthy 22-year-old man (73 kg).

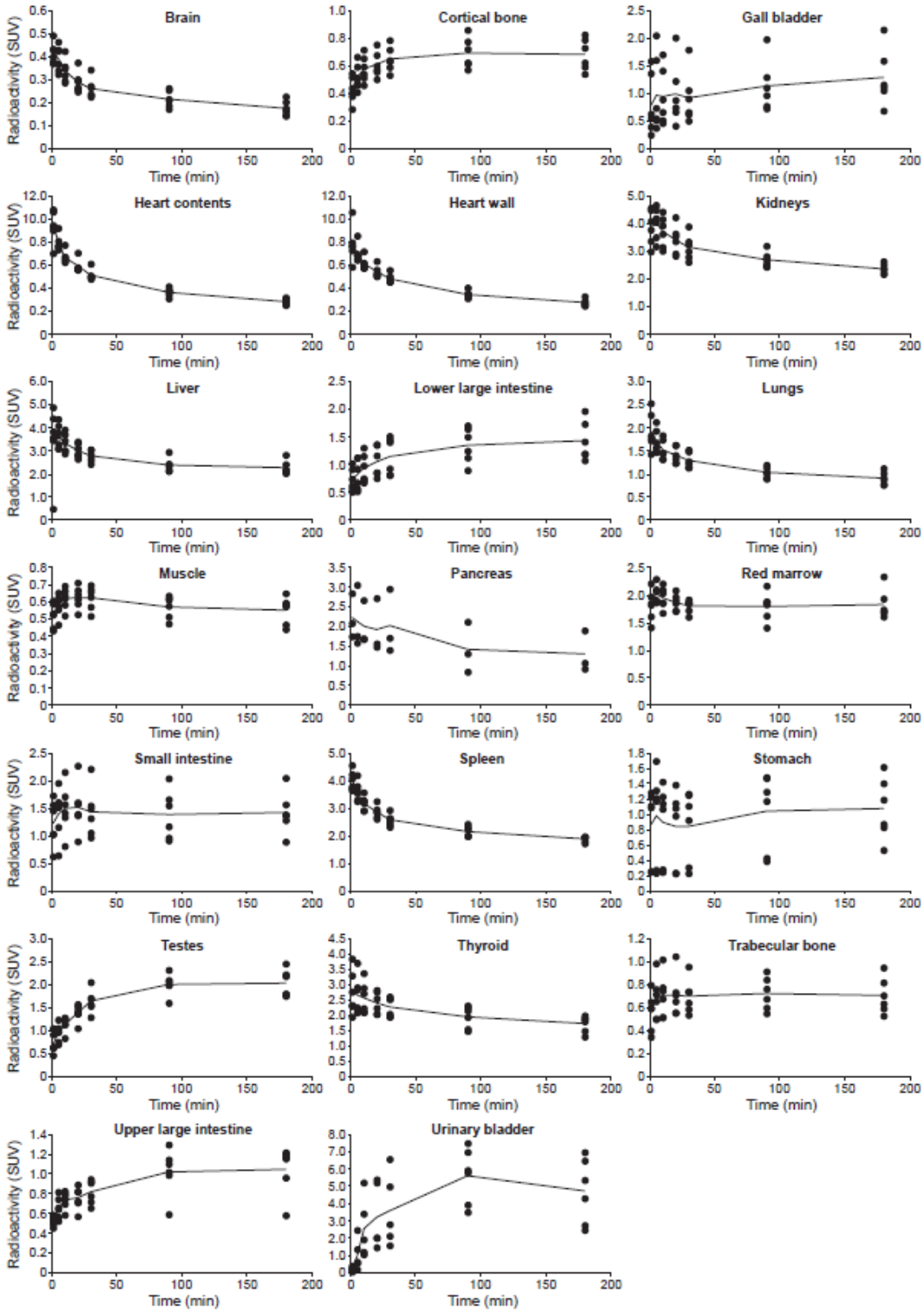

FIGURE 3. Time-activity curves of the main organs. The circles represent each individual and the line is the average.

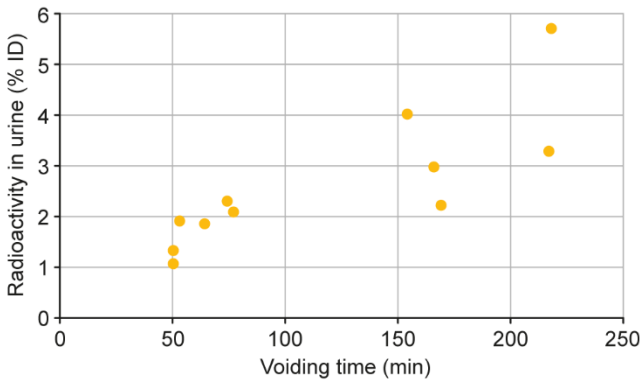

FIGURE 4. Percentage of the injected ^{68}Ga-citrate radioactivity dose (%ID) in urine as a function of time.

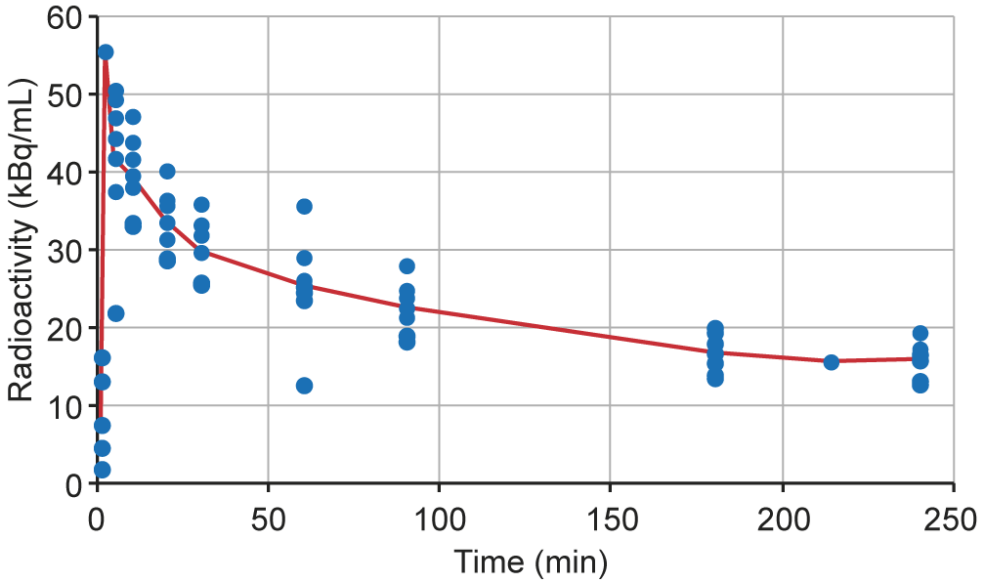

FIGURE 5. Concentration of radioactivity in arterialized venous plasma as a function of time after ^{68}Ga-citrate injection. The blue dots represent each individual and the red line is the average.

TABLE 1

Residence Times (Hours) in Source Organs After Injection of ^{68}Ga-Citrate

	Mean ± SD	COV (%)*	Range
Brain	0.008 ± 0.001	19	0.006–0.009
Gall bladder contents	0.000 ± 0.000	48	0.000–0.001
Left colon	0.002 ± 0.001	23	0.001–0.003
Small intestine	0.012 ± 0.003	27	0.007–0.016
Stomach contents	0.009 ± 0.004	38	0.004–0.013
Right colon	0.002 ± 0.001	23	0.001–0.003
Rectum	0.002 ± 0.001	25	0.001–0.003
Heart contents	0.048 ± 0.006	12	0.041–0.055
Heart wall	0.027 ± 0.004	13	0.024–0.033
Kidneys	0.020 ± 0.003	14	0.017–0.023
Liver	0.091 ± 0.017	19	0.077–0.121
Lungs	0.079 ± 0.008	10	0.066–0.088
Muscle	0.365 ± 0.043	12	0.299–0.420
Pancreas	0.005 ± 0.002	49	0.003–0.008
Red marrow	0.046 ± 0.004	10	0.038–0.052
Cortical bone	0.032 ± 0.005	15	0.026–0.040
Trabecular bone	0.009 ± 0.002	22	0.007–0.012
Spleen	0.009 ± 0.002	28	0006–0.012
Testes	0.002 ± 0.000	15	0.001–0.002
Thyroid	0.001 ± 0.000	19	0.000–0.001
Urinary bladder contents	0.021 ± 0.008	37	0.013–0.035
Remainder of the body	0.810 ± 0.033	4	0.767–0.858

*Coefficient of variation = SD/mean×100.

TABLE 2

Organ Doses and Effective Doses (mSv/MBq) After Injection of ^{68}Ga-Citrate

	Mean ± SD	COV (%)*	Range
Adrenals	0.019 ± 0.001	4	0.018–0.020
Brain	0.004 ± 0.001	12	0.004–0.005
Breasts	0.013 ± 0.000	2	0.012–0.013
Colon, left	0.021 ± 0.002	7	0.019–0.023
Colon, right	0.017 ± 0.001	4	0.016–0.018
Esophagus	0.015 ± 0.000	2	0.015–0.016
Eyes	0.011 ± 0.000	3	0.010–0.011
Gall bladder wall	0.017 ± 0.001	6	0.016–0.019
Heart wall	0.077 ± 0.008	11	0.067–0.087
Kidneys	0.036 ± 0.004	12	0.031–0.041
Liver	0.033 ± 0.005	16	0.029–0.043
Lungs	0.036 ± 0.003	8	0.031–0.040
Osteogenic cells	0.017 ± 0.001	6	0.015–0.018
Pancreas	0.020 ± 0.007	36	0.015–0.034
Prostate	0.013 ± 0.000	2	0.012–0.013
Rectum	0.020 ± 0.001	7	0.018–0.022
Red marrow	0.020 ± 0.001	5	0.019–0.022
Salivary glands	0.012 ± 0.000	3	0.011–0.012
Small intestine	0.022 ± 0.002	11	0.019–0.025
Spleen	0.032 ± 0.007	23	0.025–0.044
Stomach wall	0.024 ± 0.004	15	0.018–0.027
Testes	0.022 ± 0.003	13	0.019–0.026
Thymus	0.016 ± 0.000	2	0.016–0.017
Thyroid	0.017 ± 0.002	14	0.014–0.021
Urinary bladder wall	0.039 ± 0.010	26	0.029–0.057
Total body	0.015 ± 0.000	1	0.014–0.015
Effective dose (ICRP 60)†	0.023 ± 0.001	3	0.021–0.023
Effective dose (ICRP 103)††	0.021 ± 0.001	3	0.020–0.022

* Coefficient of variation = SD/mean×100.

†ICRP Publication 60 (*27*)

††ICRP Publication 103 (*20*).

GRAPHICAL ABSTRACT

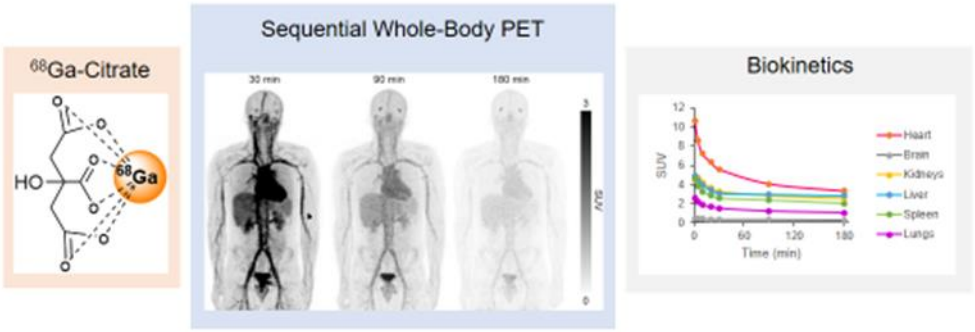

SUPPLEMENTAL DATA

SUPPLEMENTAL TABLE 1

Quality Control Data from Three Representative Batches of ^{68}Ga-Citrate

Product specifications	Limits for product release	Results
Appearance	Clear and colorless solution, free of particles	Pass
pH	3.0–7.0	4.7 ± 0.3
Radionuclidic identity	68 min ± 3 min	68.1 ± 0.2 min
Radiochemical purity	≥ 95% by iTLC*	97.3% ± 0.6
Radioactivity concentration	≥ 15 MBq/mL	44.3 ± 1.2 MBq/mL
Radionuclidic purity	≥ 99.9% ^{68}Ga ≤ 0.001% ^{68}Ge	Pass Pass
Content of ethanol	≤ 5 mg/mL	1.3% ± 1.1
Residual solvents (acetone)	≤ 5 mg/mL	0.0% ± 0.0
Sterile filter integrity	≥ 3.45 bar	4.1 ± 0.1 bar
Sterility	Sterile (no viable organisms detected)	Pass
Bacterial endotoxins	≤ 17.5 EU†/mL	1.2 ± 0.0 EU/mL

*iTLC = instant thin-layer chromatography. †EU = endotoxin units.

SUPPLEMENTAL TABLE 2

Decay-Corrected Radioactivity Concentration (SUV) of ^{68}Ga-Citrate as a Function of Time in Organs of Healthy Men

Brain

Time (h)	Time (min)	Subject #1	Subject #2	Subject #3	Subject #4	Subject #5	Subject #6	Mean	SD	Min	Max	COV
0:01:00	1.0	0.43	0.37	0.38	0.43	0.40	0.49	0.42	0.04	0.37	0.49	11 %
0:05:00	5.0	0.34	0.37	0.32	0.43	0.43	0.46	0.39	0.06	0.32	0.46	14 %
0:10:00	10.0	0.30	0.32	0.29	0.36	0.35	0.42	0.34	0.05	0.29	0.42	15 %
0:20:00	20.0	0.26	0.27	0.25	0.29	0.30	0.37	0.29	0.05	0.25	0.37	16 %
0:30:00	30.0	0.23	0.24	0.23	0.27	0.27	0.34	0.26	0.04	0.23	0.34	17 %
1:30:00	90.0	0.19	0.17	0.21	0.25	0.22	0.26	0.22	0.04	0.17	0.26	17 %
3:00:00	180.0	0.16	0.14	0.15	0.20	0.18	0.23	0.18	0.03	0.14	0.23	19 %
Organ volume (cm^3)		1505	1355	1435	1545	1662	1402	1484	111	1355	1662	7 %

Gall bladder contents

Time (h)	Time (min)	Subject #1	Subject #2	Subject #3	Subject #4	Subject #5	Subject #6	Mean	SD	Min	Max	COV
0:01:00	1.0	1.37	0.63	1.59	0.25	0.40	0.55	0.80	0.55	0.25	1.59	69 %
0:05:00	5.0	1.61	0.55	2.05	0.38	0.74	0.51	0.97	0.69	0.38	2.05	71 %
0:10:00	10.0	1.41	0.46	1.71	0.52	0.89	0.66	0.94	0.51	0.46	1.71	54 %
0:20:00	20.0	1.23	0.41	2.01	0.75	0.88	0.67	0.99	0.57	0.41	2.01	57 %
0:30:00	30.0	0.90	0.51	1.79	0.63	1.06	0.66	0.93	0.47	0.51	1.79	51 %
1:30:00	90.0	1.98	0.77	1.30	1.11	0.97	0.73	1.14	0.46	0.73	1.98	40 %
3:00:00	180.0	2.16	1.06	1.16	1.59	1.11	0.69	1.29	0.51	0.69	2.16	40 %
Organ volume (cm^3)		15	22	9	9	15	28	16	7	9	28	46 %

Lower Large Intestine (left colon & rectum)

Time (h)	Time (min)	Subject #1	Subject #2	Subject #3	Subject #4	Subject #5	Subject #6	Mean	SD	Min	Max	COV
0:01:00	1.0	0.62	0.51	0.57	1.03	0.74	0.91	0.73	0.21	0.51	1.03	28 %
0:05:00	5.0	0.68	0.56	0.52	1.12	1.13	0.93	0.82	0.27	0.52	1.13	33 %
0:10:00	10.0	0.75	0.72	0.67	1.15	1.30	0.98	0.93	0.26	0.67	1.30	28 %

0:20:00	20.0	0.85	0.75	0.86	1.36	1.37	1.16	1.06	0.27	0.75	1.37	26 %
0:30:00	30.0	0.93	0.81	0.82	1.52	1.45	1.41	1.16	0.34	0.81	1.52	29 %
1:30:00	90.0	1.13	0.90	1.25	1.71	1.65	1.50	1.36	0.32	0.90	1.71	23 %
3:00:00	180.0	1.20	1.08	1.20	1.97	1.74	1.42	1.43	0.35	1.08	1.97	25 %

Small intestine

Time (h)	Time (min)	Subject #1	Subject #2	Subject #3	Subject #4	Subject #5	Subject #6	Mean	SD	Min	Max	COV
0:01:00	1.0	1.56	1.03	0.62	1.46	1.03	1.73	1.24	0.41	0.62	1.73	33 %
0:05:00	5.0	1.55	1.16	0.64	1.52	1.96	1.61	1.41	0.45	0.64	1.96	32 %
0:10:00	10.0	1.57	1.34	0.81	1.42	2.15	1.71	1.50	0.44	0.81	2.15	30 %
0:20:00	20.0	1.58	1.37	0.90	1.39	2.27	1.60	1.52	0.45	0.90	2.27	29 %
0:30:00	30.0	1.54	1.05	0.97	1.32	2.21	1.49	1.43	0.45	0.97	2.21	31 %
1:30:00	90.0	1.66	0.92	0.96	1.17	2.04	1.55	1.38	0.44	0.92	2.04	32 %
3:00:00	180.0	1.39	1.57	0.89	1.28	2.05	1.37	1.42	0.38	0.89	2.05	27 %

Stomach contents

Time (h)	Time (min)	Subject #1	Subject #2	Subject #3	Subject #4	Subject #5	Subject #6	Mean	SD	Min	Max	COV
0:01:00	1.0	1.23	1.09	0.25	0.26	1.11	1.28	0.87	0.48	0.25	1.28	56 %
0:05:00	5.0	1.21	1.18	0.24	0.27	1.70	1.31	0.98	0.59	0.24	1.70	60 %
0:10:00	10.0	1.14	1.07	0.25	0.28	1.43	1.23	0.90	0.51	0.25	1.43	56 %
0:20:00	20.0	1.08	0.98	0.24	0.23	1.38	1.14	0.84	0.49	0.23	1.38	58 %
0:30:00	30.0	1.11	0.92	0.31	0.23	1.27	1.25	0.85	0.47	0.23	1.27	55 %
1:30:00	90.0	1.29	1.17	0.43	0.39	1.47	1.48	1.04	0.50	0.39	1.48	48 %
3:00:00	180.0	1.19	0.87	0.83	0.53	1.62	1.40	1.07	0.40	0.53	1.62	37 %

Upper large intestine (right colon)

Time (h)	Time (min)	Subject #1	Subject #2	Subject #3	Subject #4	Subject #5	Subject #6	Mean	SD	Min	Max	COV
0:01:00	1.0	0.56	0.46	0.49	0.59	0.52	0.55	0.53	0.05	0.46	0.59	9 %
0:05:00	5.0	0.64	0.57	0.52	0.75	0.82	0.66	0.66	0.11	0.52	0.82	17 %
0:10:00	10.0	0.78	0.70	0.59	0.83	0.80	0.74	0.74	0.09	0.59	0.83	12 %
0:20:00	20.0	0.82	0.73	0.57	0.89	0.82	0.71	0.76	0.11	0.57	0.89	15 %
0:30:00	30.0	0.91	0.78	0.66	0.93	0.95	0.72	0.82	0.12	0.66	0.95	15 %

1:30:00	90.0	1.15	1.02	0.59	1.30	1.10	0.99	1.03	0.24	0.59	1.30	23 %
3:00:00	180.0	1.18	0.96	0.58	1.16	1.20	1.22	1.05	0.25	0.58	1.22	24 %

Heart contents

Time (h)	Time (min)	Subject #1	Subject #2	Subject #3	Subject #4	Subject #5	Subject #6	Mean	SD	Min	Max	COV
0:01:00	1.0	9.04	9.47	9.35	10.65	7.04	10.84	9.40	1.37	7.04	10.84	15 %
0:05:00	5.0	7.37	7.70	7.69	8.11	7.53	9.23	7.94	0.68	7.37	9.23	9 %
0:10:00	10.0	6.37	6.52	6.68	6.73	6.27	7.77	6.72	0.54	6.27	7.77	8 %
0:20:00	20.0	5.81	5.66	5.69	5.61	5.69	7.08	5.93	0.57	5.61	7.08	10 %
0:30:00	30.0	5.01	5.07	4.88	5.07	4.82	6.12	5.16	0.48	4.82	6.12	9 %
1:30:00	90.0	3.85	3.45	3.68	3.80	3.11	4.16	3.67	0.36	3.11	4.16	10 %
3:00:00	180.0	3.04	2.73	2.82	3.20	2.53	2.85	2.86	0.24	2.53	3.20	8 %

Heart wall

Time (h)	Time (min)	Subject #1	Subject #2	Subject #3	Subject #4	Subject #5	Subject #6	Mean	SD	Min	Max	COV
0:01:00	1.0	7.71	7.63	7.29	10.63	5.85	7.99	7.85	1.56	5.85	10.63	20 %
0:05:00	5.0	6.84	6.46	6.55	8.56	6.84	6.93	7.03	0.77	6.46	8.56	11 %
0:10:00	10.0	5.90	5.79	5.77	7.21	5.87	6.21	6.12	0.55	5.77	7.21	9 %
0:20:00	20.0	5.27	5.08	5.05	6.35	5.26	5.60	5.44	0.49	5.05	6.35	9 %
0:30:00	30.0	4.63	4.58	4.56	5.58	4.68	5.02	4.84	0.40	4.56	5.58	8 %
1:30:00	90.0	3.51	3.27	3.27	4.04	3.13	3.55	3.46	0.33	3.13	4.04	9 %
3:00:00	180.0	2.89	2.49	2.51	3.29	2.65	2.78	2.77	0.30	2.49	3.29	11 %

Kidneys

Time (h)	Time (min)	Subject #1	Subject #2	Subject #3	Subject #4	Subject #5	Subject #6	Mean	SD	Min	Max	COV
0:01:00	1.0	3.79	4.10	3.38	4.50	3.00	4.58	3.89	0.63	3.00	4.58	16 %
0:05:00	5.0	3.51	4.07	3.18	4.68	4.21	4.51	4.03	0.58	3.18	4.68	14 %
0:10:00	10.0	3.16	3.63	3.02	4.17	3.94	4.44	3.73	0.56	3.02	4.44	15 %
0:20:00	20.0	2.92	3.37	2.84	3.64	3.56	4.24	3.43	0.51	2.84	4.24	15 %
0:30:00	30.0	2.80	3.01	2.62	3.25	3.35	3.90	3.15	0.46	2.62	3.90	14 %
1:30:00	90.0	2.48	2.54	2.44	2.83	2.69	3.20	2.70	0.29	2.44	3.20	11 %
3:00:00	180.0	2.20	2.38	2.18	2.51	2.33	2.64	2.38	0.18	2.18	2.64	8 %

Organ volume (cm^3)	326	289	320	297	375	318	321	30	289	375	9 %

Liver

Time (h)	Time (min)	Subject #1	Subject #2	Subject #3	Subject #4	Subject #5	Subject #6	Mean	SD	Min	Max	COV
0:01:00	1.0	3.59	3.84	3.46	4.89	0.47	4.41	3.45	1.55	0.47	4.89	45 %
0:05:00	5.0	3.11	3.29	3.10	4.38	4.09	3.79	3.63	0.54	3.10	4.38	15 %
0:10:00	10.0	3.00	3.02	2.88	3.92	3.71	3.45	3.33	0.43	2.88	3.92	13 %
0:20:00	20.0	2.84	2.80	2.65	3.40	3.33	3.12	3.02	0.31	2.65	3.40	10 %
0:30:00	30.0	2.71	2.58	2.42	3.06	3.04	2.84	2.78	0.25	2.42	3.06	9 %
1:30:00	90.0	2.42	2.12	2.14	2.95	2.42	2.30	2.39	0.30	2.12	2.95	13 %
3:00:00	180.0	2.41	2.10	2.03	2.82	2.12	2.18	2.28	0.30	2.03	2.82	13 %
Organ volume (cm^3)		1723	1728	1613	1715	1591	1461	1639	105	1461	1728	6 %

Lungs

Time (h)	Time (min)	Subject #1	Subject #2	Subject #3	Subject #4	Subject #5	Subject #6	Mean	SD	Min	Max	COV
0:01:00	1.0	1.78	2.28	1.83	2.53	1.43	1.73	1.93	0.40	1.43	2.53	21 %
0:05:00	5.0	1.48	1.93	1.57	2.12	1.68	1.48	1.71	0.26	1.48	2.12	15 %
0:10:00	10.0	1.32	1.74	1.45	1.84	1.45	1.32	1.52	0.22	1.32	1.84	14 %
0:20:00	20.0	1.23	1.62	1.33	1.63	1.41	1.24	1.41	0.18	1.23	1.63	13 %
0:30:00	30.0	1.15	1.52	1.23	1.49	1.27	1.13	1.30	0.17	1.13	1.52	13 %
1:30:00	90.0	0.91	1.13	1.02	1.19	1.03	0.89	1.03	0.12	0.89	1.19	11 %
3:00:00	180.0	0.76	1.12	0.87	1.01	0.91	0.77	0.91	0.14	0.76	1.12	15 %
Organ volume (cm^3)		3218	3047	3877	2824	3727	3125	3303	411	2824	3877	12 %

Muscle

Time (h)	Time (min)	Subject #1	Subject #2	Subject #3	Subject #4	Subject #5	Subject #6	Mean	SD	Min	Max	COV
0:01:00	1.0	0.59	0.61	0.53	0.43	0.45	0.53	0.52	0.07	0.43	0.61	14 %
0:05:00	5.0	0.62	0.65	0.56	0.47	0.58	0.61	0.58	0.07	0.47	0.65	11 %
0:10:00	10.0	0.66	0.69	0.58	0.52	0.62	0.64	0.62	0.06	0.52	0.69	10 %
0:20:00	20.0	0.67	0.71	0.62	0.53	0.59	0.64	0.63	0.06	0.53	0.71	10 %
0:30:00	30.0	0.67	0.70	0.63	0.52	0.57	0.66	0.62	0.07	0.52	0.70	11 %

1:30:00	90.0	0.62	0.64	0.58	0.47	0.51	0.61	0.57	0.07	0.47	0.64	11 %
3:00:00	180.0	0.57	0.65	0.59	0.44	0.47	0.59	0.55	0.08	0.44	0.65	15 %

Pancreas

Time (h)	Time (min)	Subject #1	Subject #2	Subject #3	Subject #4	Subject #5	Subject #6	Mean	SD	Min	Max	COV
0:01:00	1.0	2.84	2.09	ND	ND	ND	1.75	2.23	0.56	1.75	2.84	25 %
0:05:00	5.0	3.06	1.76	ND	ND	ND	1.59	2.14	0.80	1.59	3.06	38 %
0:10:00	10.0	2.67	1.68	ND	ND	ND	1.70	2.01	0.57	1.68	2.67	28 %
0:20:00	20.0	2.72	1.49	ND	ND	ND	1.57	1.92	0.69	1.49	2.72	36 %
0:30:00	30.0	2.95	1.41	ND	ND	ND	1.71	2.02	0.82	1.41	2.95	41 %
1:30:00	90.0	2.12	0.85	ND	ND	ND	1.32	1.43	0.64	0.85	2.12	45 %
3:00:00	180.0	1.90	0.93	ND	ND	ND	1.08	1.30	0.52	0.93	1.90	40 %

Red marrow

Time (h)	Time (min)	Subject #1	Subject #2	Subject #3	Subject #4	Subject #5	Subject #6	Mean	SD	Min	Max	COV
0:01:00	1.0	1.82	1.97	2.21	1.61	1.41	1.85	1.81	0.28	1.41	2.21	15 %
0:05:00	5.0	1.91	2.10	2.29	1.87	1.88	2.07	2.02	0.17	1.87	2.29	8 %
0:10:00	10.0	1.86	2.09	2.21	1.67	1.86	2.04	1.95	0.19	1.67	2.21	10 %
0:20:00	20.0	1.85	1.97	2.08	1.72	1.71	1.91	1.87	0.15	1.71	2.08	8 %
0:30:00	30.0	1.86	1.86	1.92	1.72	1.60	1.85	1.80	0.12	1.60	1.92	6 %
1:30:00	90.0	1.83	1.87	1.88	2.17	1.62	1.41	1.80	0.26	1.41	2.17	14 %
3:00:00	180.0	1.70	1.93	1.74	2.33	1.61	1.68	1.83	0.27	1.61	2.33	15 %

Cortical bone

Time (h)	Time (min)	Subject #1	Subject #2	Subject #3	Subject #4	Subject #5	Subject #6	Mean	SD	Min	Max	COV
0:01:00	1.0	0.41	0.52	0.38	0.44	0.29	0.55	0.43	0.09	0.29	0.55	22 %
0:05:00	5.0	0.47	0.59	0.46	0.51	0.41	0.67	0.52	0.09	0.41	0.67	18 %
0:10:00	10.0	0.54	0.65	0.51	0.60	0.46	0.72	0.58	0.09	0.46	0.72	16 %
0:20:00	20.0	0.57	0.68	0.56	0.60	0.50	0.75	0.61	0.09	0.50	0.75	15 %
0:30:00	30.0	0.59	0.72	0.64	0.63	0.53	0.79	0.65	0.09	0.53	0.79	14 %
1:30:00	90.0	0.62	0.78	0.62	0.72	0.57	0.86	0.70	0.11	0.57	0.86	16 %
3:00:00	180.0	0.59	0.73	0.62	0.79	0.54	0.83	0.68	0.11	0.54	0.83	17 %

Trabecular bone

Time (h)	Time (min)	Subject #1	Subject #2	Subject #3	Subject #4	Subject #5	Subject #6	Mean	SD	Min	Max	COV
0:01:00	1.0	0.60	0.59	0.40	0.65	0.35	0.80	0.56	0.17	0.35	0.80	30 %
0:05:00	5.0	0.66	0.72	0.50	0.76	0.50	0.98	0.69	0.18	0.50	0.98	26 %
0:10:00	10.0	0.68	0.75	0.51	0.77	0.52	1.02	0.71	0.19	0.51	1.02	27 %
0:20:00	20.0	0.65	0.73	0.55	0.71	0.56	1.05	0.71	0.18	0.55	1.05	25 %
0:30:00	30.0	0.64	0.74	0.59	0.74	0.54	0.96	0.70	0.15	0.54	0.96	21 %
1:30:00	90.0	0.68	0.76	0.60	0.84	0.55	0.91	0.72	0.14	0.55	0.91	20 %
3:00:00	180.0	0.63	0.71	0.59	0.95	0.53	0.82	0.70	0.16	0.53	0.95	22 %

Spleen

Time (h)	Time (min)	Subject #1	Subject #2	Subject #3	Subject #4	Subject #5	Subject #6	Mean	SD	Min	Max	COV
0:01:00	1.0	3.72	3.78	4.08	4.56	3.65	4.23	4.00	0.35	3.65	4.56	9 %
0:05:00	5.0	3.30	3.26	3.66	3.80	4.20	3.55	3.63	0.35	3.26	4.20	10 %
0:10:00	10.0	2.90	2.92	3.29	3.20	3.57	3.26	3.19	0.25	2.90	3.57	8 %
0:20:00	20.0	2.61	2.68	2.95	2.87	3.25	2.87	2.87	0.23	2.61	3.25	8 %
0:30:00	30.0	2.32	2.41	2.64	2.52	2.93	2.63	2.58	0.21	2.32	2.93	8 %
1:30:00	90.0	2.01	2.00	2.43	2.31	2.24	1.99	2.16	0.19	1.99	2.43	9 %
3:00:00	180.0	1.73	1.95	1.96	1.97	1.94	1.79	1.89	0.10	1.73	1.97	5 %
Organ volume (cm^3)		126	189	141	224	200	126	168	42	126	224	25 %

Testes

Time (h)	Time (min)	Subject #1	Subject #2	Subject #3	Subject #4	Subject #5	Subject #6	Mean	SD	Min	Max	COV
0:01:00	1.0	1.05	0.91	0.46	0.63	0.63	0.63	0.72	0.22	0.46	1.05	30 %
0:05:00	5.0	1.24	1.05	0.70	0.98	0.97	0.75	0.95	0.20	0.70	1.24	21 %
0:10:00	10.0	1.28	1.22	0.83	1.26	1.14	1.13	1.15	0.16	0.83	1.28	14 %
0:20:00	20.0	1.44	1.52	1.05	1.57	1.37	1.37	1.39	0.18	1.05	1.57	13 %
0:30:00	30.0	1.53	1.70	1.29	2.05	1.56	1.70	1.64	0.25	1.29	2.05	15 %
1:30:00	90.0	2.00	2.07	1.60	2.32	1.99	2.10	2.01	0.23	1.60	2.32	12 %
3:00:00	180.0	1.80	2.46	1.75	2.22	1.79	2.18	2.03	0.29	1.75	2.46	14 %

Thyroid

Time (h)	Time (min)	Subject #1	Subject #2	Subject #3	Subject #4	Subject #5	Subject #6	Mean	SD	Min	Max	COV
0:01:00	1.0	2.33	3.29	2.31	3.84	1.95	2.77	2.75	0.71	1.95	3.84	26 %
0:05:00	5.0	2.09	2.91	2.25	3.71	2.13	2.84	2.65	0.63	2.09	3.71	24 %
0:10:00	10.0	2.23	2.89	2.10	3.37	2.10	2.71	2.57	0.51	2.10	3.37	20 %
0:20:00	20.0	2.24	2.77	2.03	2.82	2.05	2.55	2.41	0.35	2.03	2.82	15 %
0:30:00	30.0	1.96	2.52	1.95	2.61	2.04	2.54	2.27	0.32	1.95	2.61	14 %
1:30:00	90.0	1.55	2.25	1.48	2.31	1.94	2.15	1.95	0.36	1.48	2.31	18 %
3:00:00	180.0	1.49	1.80	1.30	1.99	1.90	1.89	1.73	0.27	1.30	1.99	16 %
Organ volume (cm^3)		12	11	20	11	11	13	13	4	11	20	27 %

Urinary bladder contents

Time (h)	Time (min)	Subject #1	Subject #2	Subject #3	Subject #4	Subject #5	Subject #6	Mean	SD	Min	Max	COV
0:01:00	1.0	0.18	0.29	ND	0.39	0.06	0.17	0.22	0.13	0.06	0.39	58 %
0:05:00	5.0	0.56	2.47	ND	0.63	0.19	1.36	1.04	0.90	0.19	2.47	87 %
0:10:00	10.0	1.20	5.22	ND	3.42	1.06	1.92	2.57	1.76	1.06	5.22	68 %
0:20:00	20.0	1.47	5.40	ND	5.22	2.03	2.03	3.23	1.92	1.47	5.40	59 %
0:30:00	30.0	1.58	5.00	ND	6.59	2.81	2.13	3.62	2.10	1.58	6.59	58 %
1:30:00	90.0	3.51	7.00	3.94	7.51	5.80	5.94	5.62	1.60	3.51	7.51	29 %
3:00:00	180.0	2.47	6.50	2.75	5.37	4.32	6.99	4.73	1.89	2.47	6.99	40 %

COV = coefficient of variation = SD/mean×100; ND = not determined.

SUPPLEMENTAL TABLE 3

Plasma Concentration of Intravenously Administered ^{68}Ga-Citrate in Healthy Men

	C_0 (SUV g/mL)	$1/C_0$ (L/kg)*	C_{4h} (SUV g/mL)	$1/C_{4h}$ (L/kg)†
Subject #1	17.1	0.0584	6.4	0.1559
Subject #2	19.3	0.0517	ND	ND
Subject #3	15.3	0.0654	5.0	0.2010
Subject #4	18.1	0.0551	6.3	0.1600
Subject #5	15.0	0.0668	5.3	0.1882
Subject #6	18.7	0.0535	6.0	0.1660
Mean	17.3	0.0585	5.8	0.1742
SD	1.8	0.0063	0.6217	0.0195
COV (%)	11	11	11	11

SUV = standardized uptake value; COV = Coefficient of variation = SD/mean×100.

*$1/C_0$ is related to the total plasma volume.

†$1/C_{4h}$ may be related to the extracellular volume of the body.

SUPPLEMENTAL TABLE 4

Organ Doses and Effective Doses (mSv/MBq) After Injection of ^{68}Ga-Citrate According to OLINDA 1.0

	Mean ± SD	COV (%)*	Range
Adrenals	0.011 ± 0.000	2	0.011–0.011
Brain	0.004 ± 0.001	13	0.003–0.005
Breasts	0.009 ± 0.000	3	0.008–0.009
Gall bladder wall	0.013 ± 0.001	6	0.012–0.014
Lower large intestine wall	0.013 ± 0.001	7	0.012–0.014
Small intestine wall	0.017 ± 0.002	10	0.014–0.019
Stomach wall	0.018 ± 0.003	17	0.014–0.021
Upper large intestine wall	0.015 ± 0.001	7	0.013–0.016
Heart wall	0.070 ± 0.008	11	0.061–0.080
Kidneys	0.035 ± 0.004	12	0.030–0.040
Liver	0.028 ± 0.005	17	0.024–0.036
Lungs	0.040 ± 0.003	9	0.034–0.044
Muscle	0.010 ± 0.001	7	0.009–0.011
Ovaries	0.010 ± 0.000	2	0.010–0.011
Pancreas	0.021 ± 0.012	60	0.012–0.043
Red marrow	0.017 ± 0.001	6	0.015–0.018
Osteogenic cells	0.021 ± 0.001	5	0.020–0.023
Skin	0.007 ± 0.000	3	0.007–0.008
Spleen	0.026 ± 0.006	23	0.020–0.035
Testes	0.021 ± 0.003	13	0.018–0.025
Thymus	0.010 ± 0.000	2	0.010–0.011
Thyroid	0.016 ± 0.002	15	0.013–0.020
Urinary bladder wall	0.033 ± 0.009	27	0.024–0.049
Uterus	0.011 ± 0.000	3	0.011–0.011
Total body	0.013 ± 0.000	1	0.013–0.013
Effective dose (ICRP 60)†	0.020 ± 0.001	3.7	0.019–0.022
Effective dose (ICRP 103)‡	0.019 ± 0.001	3.0	0.019–0.020

* Coefficient of variation = SD/mean×100.

† ICRP Publication 60 (*27*)

‡ ICRP Publication 103 (*20*)